

# Electric arc models with non-zero residual conductance and with increased energy dissipation

ANTONI SAWICKI 

Association of Polish Electrical Engineers (NOT-SEP), Czestochowa Division  
Poland

e-mail: [sawicki.a7@gmail.com](mailto:sawicki.a7@gmail.com)

(Received: 12.03.2021, revised: 12.05.2021)

**Abstract:** This paper describes modifications of the Mayr and Cassie models of the electric arc. They include the phenomena of increased heat dissipation and non-zero residual conductance when the current passes through zero. The modified models are combined into a new hybrid model connecting them in parallel and activated by a weight function. Two cases of functional dependence of models on current intensity and instantaneous conductance are considered. Mathematical models in differential and integral forms are presented. On their basis, computer macromodels are created and simulations of processes in circuits with arc models are performed. The families of static and dynamic arc voltage and current characteristics are presented.

**Key words:** Cassie model, electric arc, hybrid model, Mayr model

## 1. Introduction

The Mayr and Cassie mathematical models of the electric arc are usually described by ordinary linear differential equations. Due to their limited possibilities to approximate dynamic arc characteristics in wide ranges of current excitation, they are sometimes combined into a hybrid model [1]. However, this approach hinders the physical interpretation of simulation results and complicates the methods of experimental determination of parameters and functions of nonlinear models [2].

Mayr and Cassie models are special cases of the more general Pentegov model [3]. In this model, the virtual state current  $i_\theta$  is introduced representing thermal states (temperature) of the thermal plasma. Due to the simplifying assumptions made, the resulting Pentegov model contains a time constant, which makes it different from the models taking into account the non-linear physical effects in the arc [4]. As a result of the weakening of its input assumptions,



a more general version of the Mayr model was created – the Pentegov model with a non-linear damping function [5].

In connection with the observed effects of local deformation of static and dynamic voltage and current characteristics [6], sometimes additional expressions are introduced to previously developed mathematical models of the arc [7]. However, this behavior can lead to a disturbance in the equation of the arc energy balance. Therefore, it is advisable to allow for the effects of characteristics deformation by introducing appropriate expressions at the initial stage of creating mathematical models [8]. The modified models so obtained are distinguished by the appearance of new quantities in the form of residual conductance and additional dissipation power [9]. Further extensions of the applications of these modified models can be achieved by combining them into a hybrid model.

In most cases, mathematical models in differential form are used to create macromodels of electric arcs [1–3]. In this way, their sequential structure is represented, consisting of a plasma column and thin electrode areas. However, for simulating the operating conditions of devices with highly distorted arcs (e.g. a gliding arc with variable column length [10]) and with higher voltage, integral models are preferred.

## 2. Modified Mayr mathematical model and its differential and integral forms

The input assumptions for creating the modified Mayr model are similar to those adopted for the classical model [3]. They can be presented as follows:

- Ohm's law

$$\frac{i}{u} = \frac{i_{\theta}}{U} = g, \quad (1)$$

- power balance equation

$$\frac{dQ}{dt} + Ui_{\theta} + P_{disM}(i_{\theta}) = ui, \quad (2)$$

- enthalpy distribution of the plasma column relative to its conductance

$$\exp\left(\frac{Q}{Q_p}\right) = \frac{g}{g_p}, \quad (3)$$

- static characteristics of the column on the assumption  $P_{disM}(i_{\theta}) = 0$

$$g = G_{1M} + \frac{i_{\theta}^2}{P_M}, \quad (4)$$

where:  $i$ ,  $u$ ,  $g$  are the instantaneous values of current, voltage and conductance;  $i_{\theta}$  is the virtual state current;  $U$  is the static voltage-current characteristic;  $G_{1M}$  is the residual conductance value corresponding to instantaneous power failure,  $Q$  is the instantaneous plasma enthalpy value;  $P_M$  is the constant power of the Mayr model,  $P_{disM}(i_{\theta})$  is the dissipation power dependent on the state current. The base quantities are  $Q_p$  enthalpy and  $g_p$  conductance. Determining conductance using the state current is equivalent to determining using the instantaneous current. In fact, it is

$g = i/u = i_\theta/U(i_\theta)$ . After substituting the expressions (1), (3) and (4) into the power balance Eq. (2) and after transformations, the modified Mayr model is obtained in the form of a differential

$$\theta_M(i_\theta) \frac{dg}{dt} + g = \frac{i^2 + P_M G_{1M}}{P_M + P_{disM}(i_\theta)}, \quad (5)$$

where the damping function is determined by the relationship

$$\theta_M(i_\theta) = \frac{Q_p}{P_M + P_{disM}(i_\theta)}, \quad (6)$$

and the quantity  $\theta_M(i_\theta)$  represents the damping function dependent on the state current. If  $P_{disM}(i_\theta) = \text{const}$  or  $P_{disM}(i_\theta) \ll P_M$ , then the damping function can be approximately taken as a constant quantity  $\theta_M(i_\theta) = \theta_M = \text{const}$ .

The  $G_{1M}$  value affects the angle of the tangent to the voltage-current characteristic at the beginning of the coordinate system ( $I, U$ ). Let symbol  $I_M = \sqrt{P_M G_M}$  represent the current, which is the abscissa of the arc ignition point. The dissipation power is very often assumed to be dependent on the current  $P_{disM}(i)$  [11] and only sometimes the dependence of conductance  $P_{disM}(g)$  is used. This leads to differential equations with slightly different forms.

Equation (5) can be converted to an integral form

$$g = g_0 \exp \left[ \frac{1}{\theta_M} \int_0^t \left( \frac{i^2 + P_M G_{1M}}{P_M + P_{disM}(i_\theta)} \frac{1}{g} - 1 \right) d\tau \right]. \quad (7)$$

Two cases can be considered here:

– if  $G_{1M} = 0$  S, then

$$g = g_0 \exp \left[ \frac{1}{\theta_M} \int_0^t \left( \frac{ui}{P_M + P_{disM}(i_\theta)} - 1 \right) d\tau \right], \quad (8)$$

– if  $P_{disM}(i_\theta) = 0$  W, then

$$g = g_0 \exp \left[ \frac{1}{\theta_M} \int_0^t \left( \frac{ui}{P_M} - 1 + \frac{G_{1M}}{g} \right) d\tau \right]. \quad (9)$$

### 3. Modified Cassie mathematical model and its differential and integral forms

The input assumptions for creating the modified Cassie model are similar to those adopted for the classical model [3]. They can be presented as follows:

- Ohm's law (1),
- power balance equation

$$\frac{dQ}{dt} + UI + P_{disC}(i_\theta) = ui, \quad (10)$$

- distribution of plasma enthalpy in relation to its conductance

$$\frac{Q}{Q_p} = \frac{g}{g_p}, \quad (11)$$

- static characteristics of the column with the assumption  $P_{disC}(i_\theta) = 0$

$$g = G_{1C} + \frac{I}{U_C}, \quad (12)$$

where:  $G_{1C}$  is the residual conductance corresponding to instantaneous power failure,  $U_C$  is the Cassie's constant voltage value,  $P_{disC}(i_\theta)$  is the instantaneous value of dissipated power depending on the current. After substituting expressions (1), (11) and (12) into power balance Eq. (10) and after appropriate transformations, a modified Cassie model can be obtained in the form of a differential equation

$$\theta_C \frac{dg^2}{dt} + (g - G_{1C})^2 = \frac{i^2 - P_{disC}(i_\theta)g}{U_C^2}, \quad (13)$$

where the time constant is determined by

$$\theta_C = \frac{Q_p}{2g_p U_C}. \quad (14)$$

As can be seen, this is a non-linear model. Unlike the classic Cassie model, there may be (if  $P_{disC}(i_\theta) = 0$ ) a reduction of the ignition voltage to zero. The  $G_{1C}$  value affects the angle of the tangent to the voltage-current characteristic at the beginning of the coordinate system ( $I, U$ ). Here, too, the dissipation power dependence on the  $P_{disC}(i_\theta)$  current intensity is often used [11]. Only sometimes  $P_{disC}(g)$  conductance dependence is used [9]. This leads to differential equations with slightly different forms.

Equation (13) can be converted to an integral form

$$g = g_0 \exp \left[ \frac{1}{2\theta_C} \int_0^t \left( \frac{u^2 - \frac{P_{disC}(i_\theta)}{g}}{U_C^2} - \left( 1 - \frac{G_{1C}}{g} \right)^2 \right) d\tau \right]. \quad (15)$$

Two cases can be considered here:

- if  $G_{1C} = 0$  S, then

$$g = g_0 \exp \left[ \frac{1}{2\theta_C} \int_0^t \left( \frac{u^2 - \frac{P_{disC}(i_\theta)}{g}}{U_C^2} - 1 \right) d\tau \right], \quad (16)$$

- if  $P_{disC}(i_\theta) = 0$  W, then

$$g = g_0 \exp \left[ \frac{1}{2\theta_C} \int_0^t \left( \frac{u^2}{U_C^2} - \left( 1 - \frac{G_{1C}}{g} \right)^2 \right) d\tau \right]. \quad (17)$$

#### 4. Modified hybrid mathematical model and its differential and integral form

In order to create a hybrid model, two passive components are connected in parallel with the conductances described by the modified Mayr (5) and Cassie (13) models with the assumption  $G_{1C} = 0$  S

$$g_M = g = \frac{i^2 + P_M G_{1M}}{P_M + P_{disM}(i_\theta)} - \theta_M \frac{dg}{dt}, \quad \text{if } |i| < I_0, \quad (18)$$

$$g_C = g = \frac{ui - P_{disC}(i_\theta)}{U_C^2} - 2\theta_C \frac{dg}{dt}, \quad \text{if } |i| \geq I_0, \quad (19)$$

where  $I_0$  is the current, which corresponds to a smooth switching between models. Models are activated by the weight function  $\varepsilon(i_\theta)$

$$g = \varepsilon(i_\theta)g_M + [1 - \varepsilon(i_\theta)]g_C. \quad (20)$$

This function takes the boundary values  $\varepsilon(0) = 1$  and  $\varepsilon(\infty) = 0$ . The argument to this function is most typically the instantaneous current, resulting in the relationship  $\varepsilon(i)$ . Sometimes due to the time shift of the arc dynamic characteristics relative to the current, it is more advantageous to use the conductance  $g$  as an argument of the weight function  $\varepsilon(g)$ . The modified hybrid model can be presented in the differential form

$$g = \varepsilon(i_\theta) \frac{i^2 + P_M G_{1M}}{P_M + P_{disM}(i_\theta)} + [1 - \varepsilon(i_\theta)] \frac{ui - P_{disC}(i_\theta)}{U_C^2} - \theta(i_\theta) \frac{dg}{dt}, \quad (21)$$

or after introducing  $I_M^2 = P_M G_{1M}$  the following can be obtained

$$g = \varepsilon(i_\theta) \frac{i^2 + I_M^2}{P_M + P_{disM}(i_\theta)} + [1 - \varepsilon(i_\theta)] \frac{ui - P_{disC}(i_\theta)}{U_C^2} - \theta(i_\theta) \frac{dg}{dt}. \quad (22)$$

If the damping function is dependent on the instantaneous current, we obtain

$$\theta(i) = \begin{cases} \theta_M, & \text{if } i < I_0 \\ 2\theta_C, & \text{if } i \geq I_0 \end{cases}, \quad (23)$$

and if it is dependent on the conductance  $g$  we obtain

$$\theta(g) = \begin{cases} \theta_M, & \text{if } g < G_0 \\ 2\theta_C, & \text{if } g \geq G_0 \end{cases}. \quad (24)$$

The double value of the time constant  $2\theta_C$  results from the transformation of the original Cassie linear model [1]. Based on the results of physical experiments [4] and computer simulations [1], it can be assumed that inequality occurs  $\theta_M \gg 2\theta_C$ .

Due to the weight function, the residual conductance in the Cassie submodel ( $G_{1C} = 0$  S) was omitted. In the case of simplified sub-models, assuming the condition ( $P_{disM} = 0$  W,  $P_{disC} = 0$  W)

and comparing static characteristics (4) and (12), one can obtain the formula for the switching current of the sub-models

$$I_0 = \frac{1}{2} \left( \frac{P_M}{U_C} + \sqrt{\left( \frac{P_M}{U_C} \right)^2 - 4P_M G_{1M}} \right). \quad (25)$$

If, at the intersection point of the static characteristics of the sub-model, the influence of the residual conductance of the Mayr sub-model ( $G_{1M} = 0$  S) is additionally omitted, then we obtain a simple relationship  $I_0 = P_M U_C^{-1}$ . The point  $(I_0, U_C)$  will correspond to the  $G_0$  conductance of the switching between the sub-models

$$G_0 = \frac{I_0}{U_C}. \quad (26)$$

The differential model, (22), can be converted to an integral form

$$g = g_0 \exp \left\{ \int_0^t \frac{1}{\theta(i_\theta)} \left[ \varepsilon(i_\theta) \frac{ui + I_M^2/g}{P_M + P_{disM}(i_\theta)} + [1 - \varepsilon(i_\theta)] \frac{u^2 - P_{disC}(i_\theta)/g}{U_C^2} - 1 \right] d\tau \right\}. \quad (27)$$

Depending on the type of electric arc and the required accuracy of approximation, the function  $\varepsilon$  may have a different analytical form. In [1], the weight function obtained using the Gaussian curve was assumed

$$\varepsilon'(i) = \exp\left(-\frac{i^2}{I_0^2}\right). \quad (28)$$

It corresponds to weight function in the form

$$\varepsilon''(g) = \exp\left(-\frac{g}{g_0}\right). \quad (29)$$

Due to the significant difference in the time values of sub-models (5) and (13) and the strong physical non-linearity of the damping function [4], it is approximated by the function  $\theta(i_\theta)$ . It can be expressed by dependence [1]

$$\theta'(i) = \theta_{i0} + \theta_{i1} \exp(-\alpha_i |i|) \approx \begin{cases} \theta_{i1}, & \text{if } |i| \text{ is low} \\ \theta_{i0}, & \text{if } |i| \text{ is large} \end{cases}, \quad (30)$$

where  $\alpha_i > 0$  s,  $\theta_{i1} > \theta_{i0} > 0$  s are the constant approximation coefficients. A variant of the damping function often more similar to real physical phenomena can be given in the following form:

$$\theta''(g) = \theta_{g0} + \theta_{g1} \exp(-\alpha_g g) \approx \begin{cases} \theta_{g1}, & \text{if } g \text{ is low} \\ \theta_{g0}, & \text{if } g \text{ is large} \end{cases}, \quad (31)$$

where  $\alpha_g > 0$  s,  $\theta_{g1} > \theta_{g0} > 0$  s are the constant approximation coefficients. In practice, it is usually assumed to simultaneously depend on two functions of the hybrid model (i.e. the weight and damping functions) either on current or on conductance.

In quasi-static states of the electric arc burning while the current is being gradually reduced, after it reaches the critical value of  $I_{\min}$ , loss of stability and quenching of the arc occurs. If external factors supporting ionized plasma in the inter-electrode area do not work (e.g. auxiliary arc, strong laser radiation, high electric field intensity), then the residual conductance values are zero ( $G_{1M} = 0$  S,  $G_{1C} = 0$  S).

## 5. Families of model static voltage-current characteristics of the modified Mayr model of the electric arc

On the basis of assumptions (1) and (4) of the modified Mayr model, a formula for the voltage on the column can be obtained, when no distortions on the part of the dissipated power  $P_{disM}(i_\theta) = 0$  occur, corresponding to the static characteristics when  $i_\theta = I$

$$U = \frac{I}{G_{1M} + \frac{I^2}{P_M}}. \quad (32)$$

Curves of static characteristics of the modified Mayr model (32) are shown in Fig. 1. The impact of gradual changes in  $P_M$  power and residual conductance  $G_{1M}$  is considered here. The range of current changes is from 0 to 20 A. It can be seen that an increase in the  $P_M$  parameter leads to an increase in characteristics and a slight shift to the right, which results in an increase in arc power and voltage (ignition) extremes. It is achieved with slightly higher currents. However, an increase in  $G_{1W}$  conductance reduces the ignition voltage. This is accompanied by a shift to the right of the extreme voltage values.

However, under the conditions of increased power dissipation, Formula (5) is obtained

$$U = \frac{I(P_M + P_{disM}(I))}{I^2 + P_M G_{1M}}. \quad (33)$$

So, Formula (32) is a special case of Formula (33).

Assume that the residual conductance  $G_{1M} = 0$  S. Then Formula (33) simplifies to the form

$$UI = P_M + P_{disM}(I). \quad (34)$$

Assume static voltage-current characteristics in the form

$$U = \frac{P_M}{I} + a_{M1}I + a_{M2}I^2, \quad (35)$$

where constant coefficients are expressed in units:  $a_{i1}$  in  $\Omega$ ,  $a_{i2}$  in  $\text{VA}^{-2}$ . Then the characteristics of additional dissipated power will be described by

$$P_{disM}(I) = I(a_{M1}I + a_{M2}I^2). \quad (36)$$

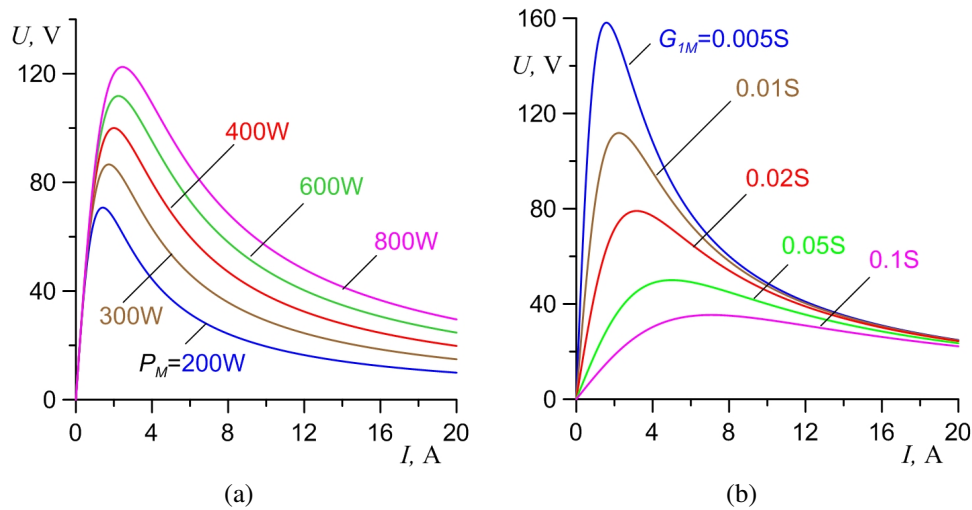


Fig. 1. Model static voltage-current characteristics families described by Formula (29): (a) depending on changes in the  $P_M$  parameter ( $G_{1M} = 0.01$  S); (b) depending on changes in the  $G_{1M}$  parameter ( $P_M = 500$  W)

The  $G_{1M}$  residual conductance has a significant impact on the shape of the voltage-current characteristics in the range of very small current values. However, raising these characteristics is accompanied by an increased  $P_{disM}$  dissipation power in the range of strong current [6]. Therefore, if you consider Formula (36), then from (33) you can get the explicit form of static characteristics

$$U = \frac{I \left[ P_M + I (a_{M1}I + a_{M2}I^2) \right]}{I^2 + P_M G_{1M}}. \quad (37)$$

Figure 2 shows the graphs of model static characteristics (37) of the modified Mayr model. Here, the effects of gradual changes of selected parameters were taken into account:  $P_M$  power, residual conductance  $G_{1M}$  and approximation coefficients of additional dissipated power  $a_{M1}$  and  $a_{M2}$ . The range of current changes is from 0 to 20 A. It can be seen that the increase in the  $P_M$  power index leads to an increase in extreme voltage values and their shift towards higher currents, which results in an increase in arc power. An increase in residual conductance leads to a decrease in extreme voltage values, which in turn leads to a reduction in power in the range of weaker currents. The increase in the value of the  $a_{M1}$  factor causes the voltage curves to rise in the range of strong currents. At the same time, these characteristics become close to linear. The extreme voltage value only increases slightly. The increase of the  $a_{M2}$  coefficient also causes the increase of the characteristics in the high-current range. At the same time, these characteristics become close to parabolic. In comparison with the previous case, the extreme voltage value is even smaller.

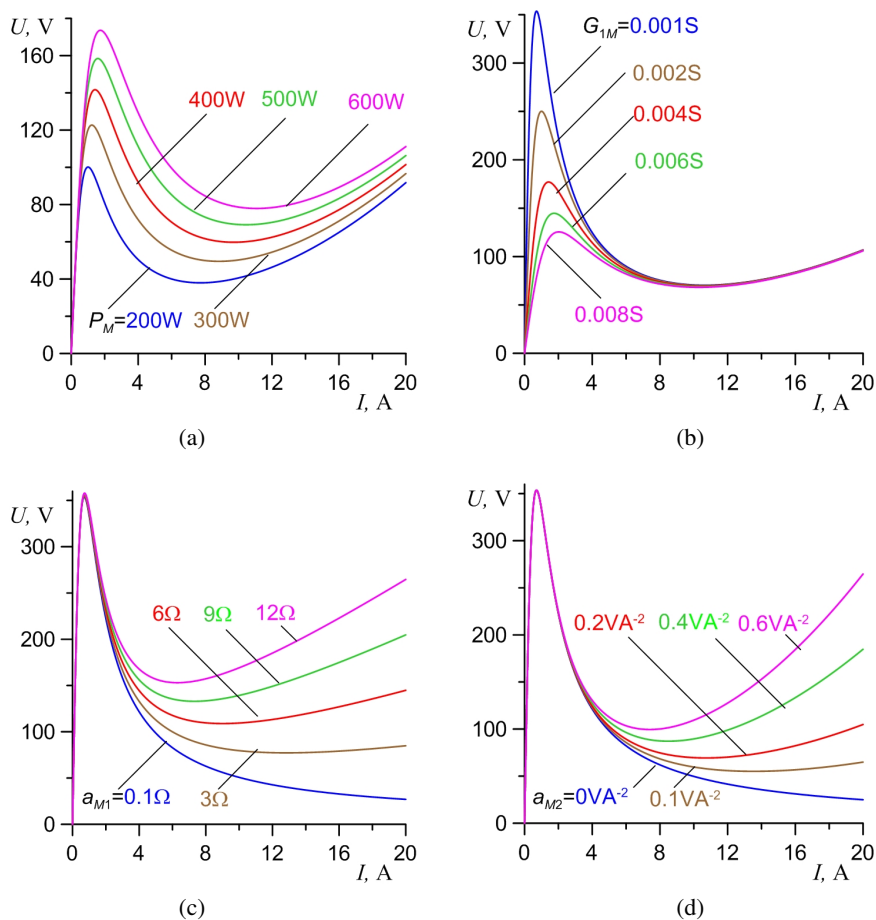


Fig. 2. The families of model static voltage-current characteristics of the modified Mayr model described by Formula (36): (a) depending on changes in the parameter  $P_M$  ( $G_{1M} = 0.005$  S,  $a_{M1} = 0.1$  V,  $a_{M2} = 0.2$   $\Omega$ ); (b) depending on changes in residual conductance  $G_M$  ( $P_M = 500$  W,  $a_{M1} = 0.1$  V,  $a_{M2} = 0.2$   $\Omega$ ); (c) depending on changes in the approximation parameter  $a_{M1}$  ( $P_M = 500$  W,  $G_{1M} = 0.001$  S,  $a_{M2} = 0$   $\Omega$ ); (d) depending on changes in the approximation parameter  $a_{M2}$  ( $P_M = 500$  W,  $G_{1M} = 0.001$  S,  $a_{M1} = 0$  V)

## 6. Families of model static voltage-current characteristics of the modified Cassie model of the electric arc

On the basis of Formulas (1) and (12) the assumed dependence on the voltage of the modified Cassie model can be obtained, representing the static characteristics for  $i_\theta = I$ , when there is no distortion on the part of the dissipated power from the column

$$U = \frac{I}{G_{1C} + \frac{I}{U_C}}. \quad (38)$$

Graphs of model static characteristics, determined by Formula (38), of the modified Cassie model are shown in Fig. 3. The impact of gradual changes in  $U_C$  voltage and residual conductance  $G_{1C}$  is included here. The range of current changes is from 0 to 200 A. As can be observed, the gradual increase in voltage  $U_C$  leads to an increase in characteristics while maintaining the effect of reducing the ignition voltage. In contrast, the increase in residual conductance causes a decrease in the angle of the tangent to the static characteristic at the beginning of the coordinate system while maintaining the voltage value in the high-current range.

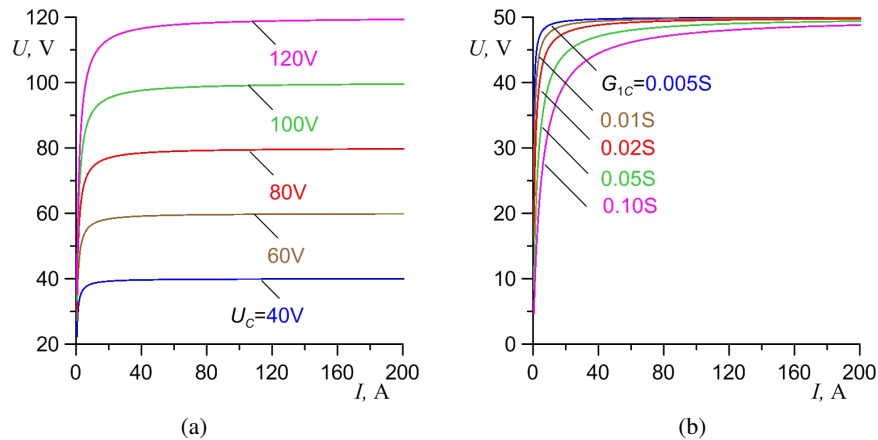


Fig. 3. Model static voltage-current characteristics families of the modified Cassie model described by Formula (37): (a) depending on changes in the  $U_C$  parameter ( $G_{1C} = 0.01$  S); (b) depending on changes in the  $G_{1C}$  parameter ( $U_{1C} = 50$  V)

If the additional dissipating power is taken into account, then it is possible to obtain the implicit formula for the static voltage of the arc column on the basis of (13).

$$\left(\frac{I}{U} - G_{1C}\right)^2 = \frac{I^2 - P_{disC}(I) \frac{I}{U}}{U_C^2}. \quad (39)$$

Thus, Formula (38) is a special case of (39) in the absence of additional dissipation. Since the analysis of Formula (39) is quite complex, we will consider its simple cases.

Suppose the residual conductance is  $G_{1C} = 0$  S. Then Formula (39) becomes simplified as

$$\left(\frac{I}{U}\right)^2 = \frac{I^2 - P_{disC}(I) \frac{I}{U}}{U_C^2}. \quad (40)$$

Let the given static characteristics of the arc model have a general form

$$U = U_C + U_d(I). \quad (41)$$

Then after substituting (41) into (40) and solving this equation with respect to  $P_{disC}(I)$  we get

$$P_{disC}(I) = \frac{2U_C + U_d(I)}{U_C + U_d(I)} U_d(I) I, \quad (42)$$

which indicates the possibility that the impact of modifying the model static voltage-current characteristics on the additional dissipated power is more complicated than it follows from Mayr model. Using this relationship ensures that the arc column's power balance is satisfied  $P_{col}(I) = P_C(I) + P_{dis}(I)$ .

Let's assume static voltage-current characteristics in a special form

$$U(I) = U_C + a_{C1}I + a_{C2}I^2, \quad (43)$$

where constant coefficients are expressed in units:  $a_{C1}$  in  $\Omega$ ,  $a_{C2}$  in  $\text{VA}^{-2}$ . Then, based on (41), the characteristics of additional dissipated power will be approximated by the relationship

$$P_{disC}(I) = \frac{2U_C + a_{C1}I + a_{C2}I^2}{U_C + a_{C1}I + a_{C2}I^2} (a_{C1}I + a_{C2}I^2) I. \quad (44)$$

The  $G_{1C}$  residual conductance has a significant impact on the shape of the model voltage-current characteristics in the range of very small current values. However, increasing these characteristics in the range of strong current is accompanied by increased  $P_{disC}$  dissipation power [5].

Figure 4 shows families of model static voltage-current and power-current characteristics. To obtain them, dependencies (43) and (44) were used. They indicate that it is possible to approximate the characteristics of high-current arcs using the formulas presented.

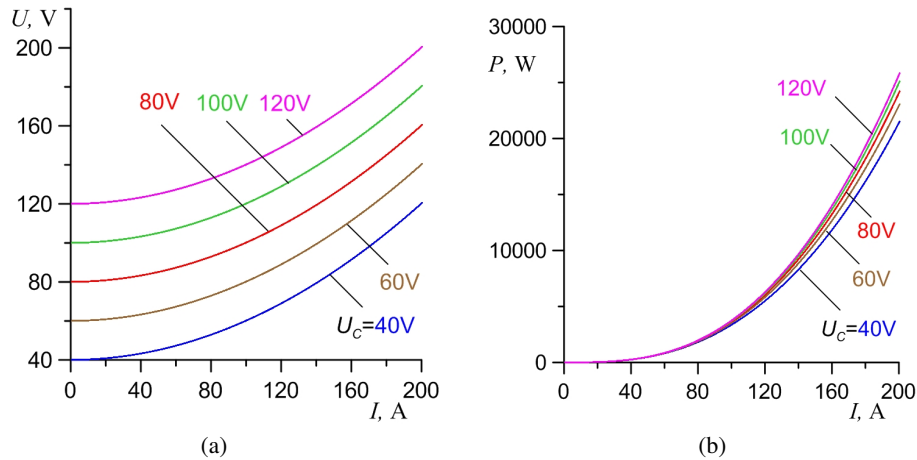


Fig. 4. Electrical characteristics of the arc described by the modified Cassie model with increased dissipation power: (a) model voltage-current characteristics; (b) power-current characteristics ( $G_{1C} = 0$  S,  $a_{C1} = 0.001 \Omega$ ,  $a_{C2} = 0.002 \text{ VA}^{-2}$ )

The formula determining the static characteristics of a hybrid model depends on the form of the weight function and is fairly complex. In the case of increased dissipation power, described by functional dependency (36) or (44), it becomes even more complicated. Therefore, in further considerations the problem of analytical determination of static characteristics of such models was omitted.

## 7. Results of simulation tests of dynamic states in a circuit with modified models of electric arc

Simulations were carried out to test the approximation potential of the proposed modified mathematical models of the electric arc. To this end, macromodels of the arc were created in several versions. In two equivalent versions, either the differential form or the integral form of the mathematical model was used. Non-linear functions ( $\varepsilon$ ,  $\theta$ ) in these macromodels were dependent on either the electric current  $i_\theta$  or the arc column conductance value  $g$ . A mixed dependence of non-linear functions on  $g$  and  $i_\theta$  was also used. The sum of the electrode voltage drops  $U_{AC} = 16$  V. A current source generating a 50 Hz sine wave was used as forcing in the arc circuit. For the modified Mayr model, the current of 20 A was used, and for the modified Cassie model and the modified Mayr–Cassie model, the current of 200 A was used. The calculations were made using the standard trapezoids rule method of numerical integration (ode23t mod stiff/Trapezoidal) with a variable step (max. step size  $10^{-4}$ , min step size  $10^{-6}$ ).

Unlike static characteristics, currents with a variable flow direction are most often used to display dynamic characteristics. If we use alternating current (and not the state current  $i_\theta$ ) in the formulas for mathematical models of the arc, then its properties should be taken into account in the functions determining the additional dissipated power ( $P_{disM}(|i|)$ ,  $P_{disC}(|i|)$ ).

Figure 5 shows the families of dynamic voltage-current characteristics obtained using the modified Mayr model in equivalent differential (5) and integral (7) forms. It can be seen that the increase in  $P_M$  power leads to a change in the shape of the characteristics while maintaining their central symmetry. The ignition voltage and RMS voltage increase. The increase in  $G_{1M}$  residual conductance causes changes in the shape of the characteristics, still preserving the central symmetry. A reduction in ignition voltage and arc RMS voltage is obtained. An increase in the  $a_{M1}$  approximation coefficient leads to loop deformation, with the central symmetry being preserved. Fragments of voltage characteristics rise, especially in the range of stronger currents. The ignition voltage increases slightly. In the case of  $a_{M2}$  increase, the ignition voltage increases only slightly. However, the largest increase in the instantaneous voltage value occurs in the range of stronger currents. To obtain the characteristics shown in Figs. 5(a) and 5(b), macromodels were created based on the differential models. Macromodels created on the basis of equivalent models in the integral form were used to obtain the characteristics shown in Figs. 5(c) and 5(d).

Figure 6 shows the families of dynamic voltage-current characteristics obtained using the modified Cassie model in the equivalent differential (13) and integral (15) forms. It can be seen that the increase in voltage  $U_C$  leads to a change in the shape of the characteristics while maintaining their central symmetry. The ignition voltage and RMS voltage increase. The increase in  $G_{1C}$  residual conductance causes changes in the shape of the characteristics, preserving the central symmetry. A reduction in ignition voltage and arc RMS voltage is obtained. An increase in the approximation coefficient  $a_{C1}$  leads to loop deformation while maintaining their central symmetry. Curves rise, especially in the stronger current range. The ignition voltage increases slightly. In the case of  $a_{C2}$  increase, the shape the characteristics changes, maintaining their central symmetry. The ignition voltage in the low current range increases slightly. However, the largest increase in the instantaneous voltage value occurs in the range of stronger currents. It may even exceed the ignition voltage in the low current range. To obtain the characteristics shown in Figs. 6(a) and 6(b), macromodels based on differential models were used, and for

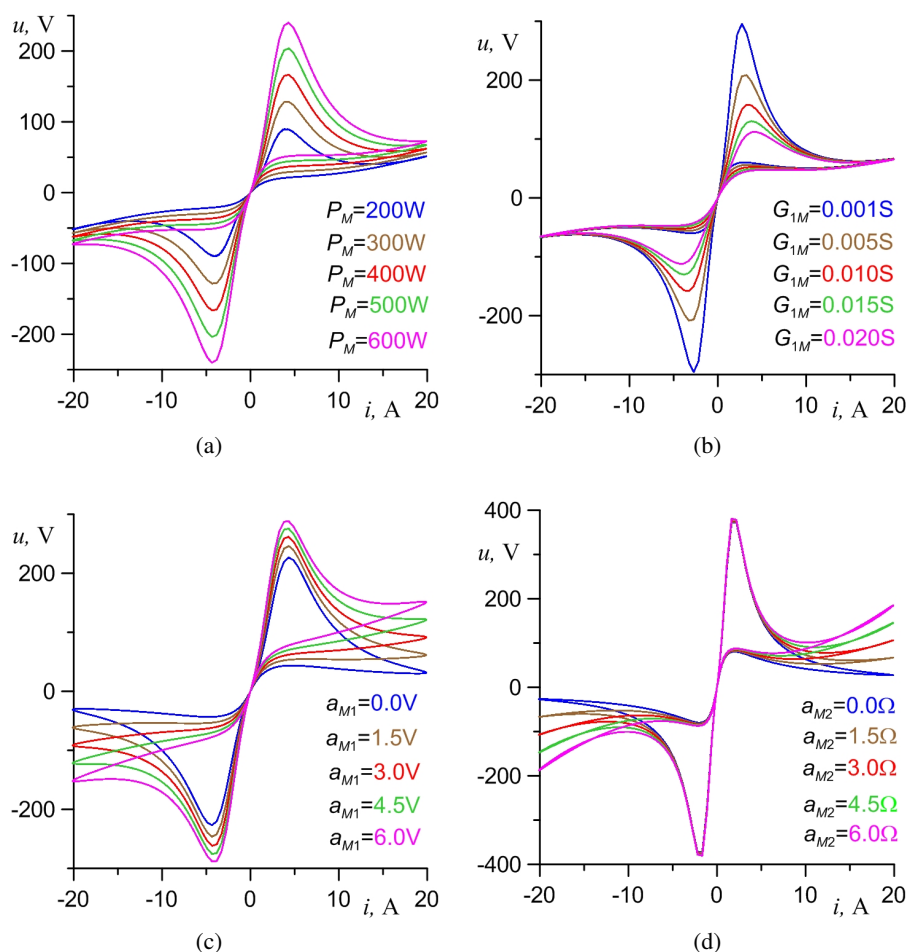


Fig. 5. Families of dynamic voltage and current characteristics of an electric arc described by the modified Mayr model: (a) in the differential form with parameters ( $G_{1M} = 0.01\text{ S}$ ,  $a_{M1} = 0.1\text{ V}$ ,  $a_{M2} = 0.1\ \Omega$ ,  $\theta_M = 5 \cdot 10^{-4}\text{ s}$ ); (b) in the differential form with parameters ( $P_M = 500\text{ W}$ ,  $a_{M1} = 0.1\text{ V}$ ,  $a_{M2} = 0.1\ \Omega$ ,  $\theta_M = 3 \cdot 10^{-4}\text{ s}$ ); (c) in the integral form with parameters ( $P_M = 600\text{ W}$ ,  $G_{1M} = 0.001\text{ S}$ ,  $a_{M2} = 0\text{ V}$ ,  $\theta_M = 5 \cdot 10^{-4}\text{ s}$ ); (d) in the integral form with parameters ( $P_M = 500\text{ W}$ ,  $G_{1M} = 0.001\text{ S}$ ,  $a_{M1} = 0.1\text{ V}$ ,  $\theta_M = 2 \cdot 10^{-4}\text{ s}$ )

the characteristics shown in Figs. 6(c) and 6(d) macromodels were created based on equivalent models in the integral form.

Figure 7 shows the families of dynamic voltage-current characteristics obtained using the modified Mayr–Cassie hybrid model in the equivalent differential (22) and integral (27) forms. The values of nonlinear functions  $\varepsilon'$ ,  $\theta'$  depended on the current according to (28) and (30). It can be observed that the increase in  $P_M$  power leads to a change in the shape of the characteristics while maintaining their central symmetry. First of all, the ignition voltage is increased. Increasing

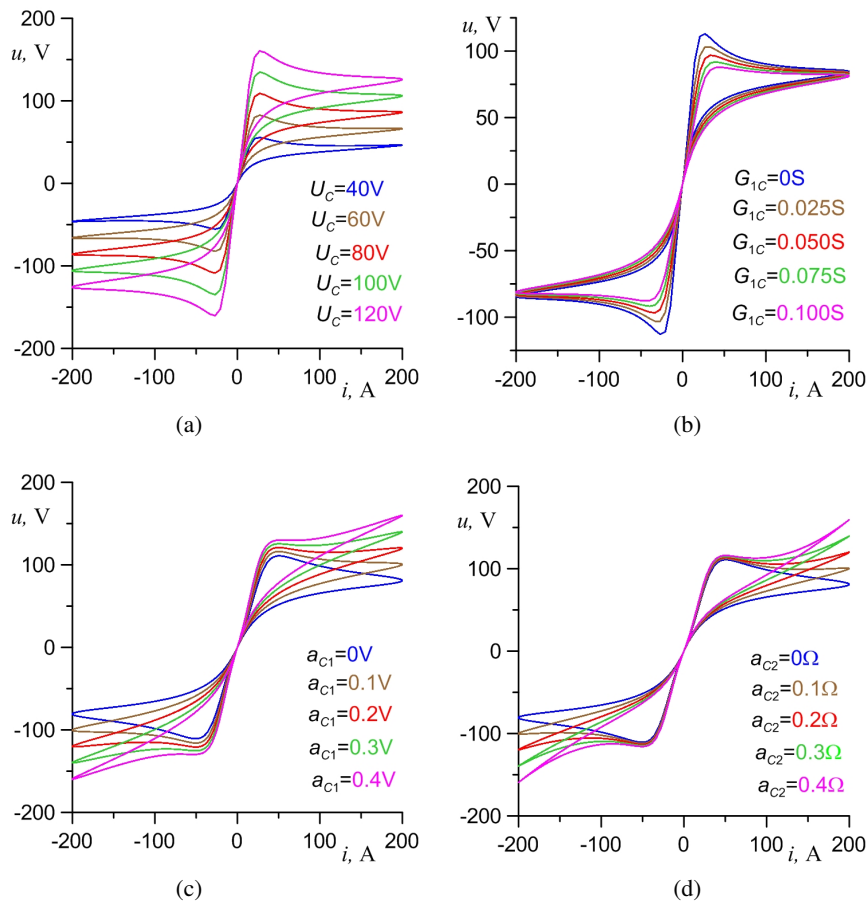


Fig. 6. Families of dynamic voltage and current characteristics of an electric arc described by a modified Cassie model: (a) in the differential form with parameters ( $G_{1C} = 0.01\text{ S}$ ,  $a_{C1} = 0.001\text{ V}$ ,  $a_{C2} = 0.00015\text{ }\Omega$ ,  $\theta_C = 2 \cdot 10^{-4}\text{ s}$ ); (b) in the differential form with parameters ( $U_C = 80\text{ V}$ ,  $a_{C1} = 0.001\text{ V}$ ,  $a_{C2} = 0.0001\text{ }\Omega$ ,  $\theta_C = 2 \cdot 10^{-4}\text{ s}$ ); (c) in the integral form with parameters ( $U_C = 80\text{ V}$ ,  $G_{1C} = 0.01\text{ S}$ ,  $a_{C2} = 0\text{ }\Omega$ ,  $\theta_C = 2 \cdot 10^{-4}\text{ s}$ ); (d) in the integral form with parameters ( $U_C = 80\text{ V}$ ,  $G_{1C} = 0.01\text{ S}$ ,  $a_{C1} = 0.1\text{ V}$ ,  $\theta_C = 2 \cdot 10^{-4}\text{ s}$ )

the  $U_C$  voltage causes changes in the shape of the characteristics while maintaining their central symmetry. An increase in ignition voltage and RMS voltage is obtained. The value of the additional dissipated power depended on the current intensity as expressed by Formulas (36) and (44). Constant and relatively small values of  $a_{M1}$  and  $a_{M2}$  coefficients were used. However, the  $a_{C1}$  and  $a_{C2}$  coefficients changed significantly. As a result of the simulations, analogous results were obtained as in the case of the Cassie model in the high-current range. To obtain the characteristics shown in Figs. 7(a) and 7(b), macromodels based on models in the differential form were used, whereas to obtain the characteristics shown in Figs. 7(c) and 7(d), macromodels were created based on equivalent models in the integral form.

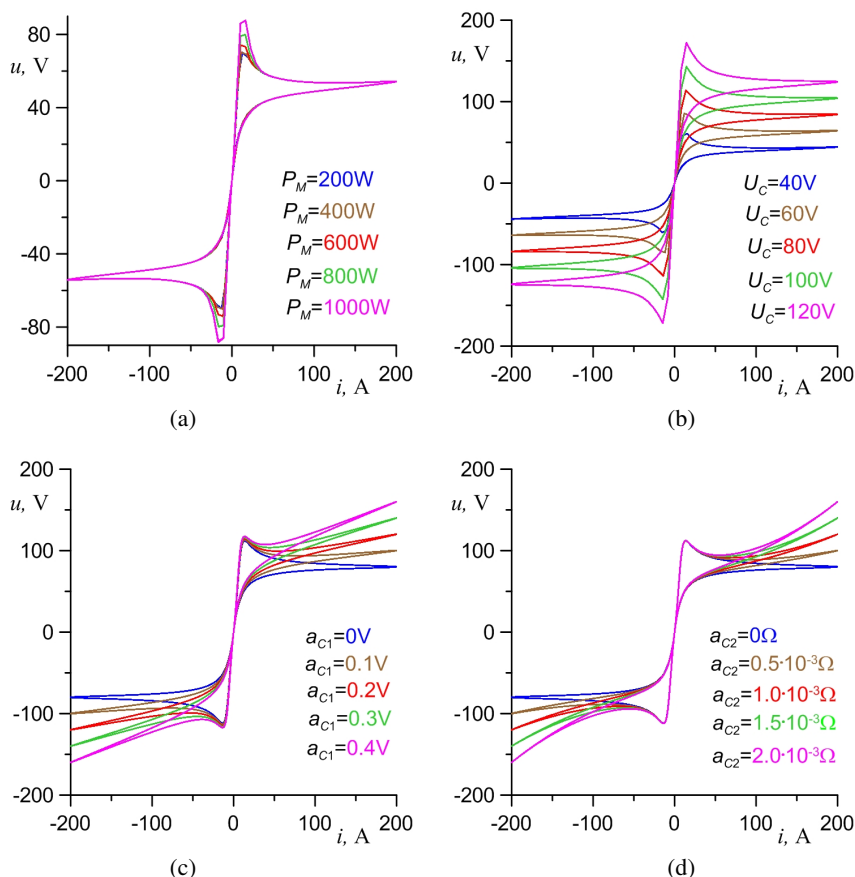


Fig. 7. Voltage-current dynamic characteristics of an electric arc described by a modified Mayr-Cassie hybrid model: (a) in the differential form with parameters ( $U_C = 50$  V,  $G_{1M} = 0.001$  S,  $a_{M1} = 0.01$  V,  $a_{M2} = 0.01$   $\Omega$ ,  $a_{C1} = 0.001$  V,  $a_{C2} = 0.0001$   $\Omega$ ,  $\theta_0 = 1 \cdot 10^{-5}$  s,  $\theta_1 = 2 \cdot 10^{-4}$  s,  $\alpha = 0.001$ ); (b) in the differential form with parameters ( $P_M = 500$  W,  $G_{1M} = 0.001$  S,  $a_{M1} = 0.01$  V,  $a_{M2} = 0.01$   $\Omega$ ,  $a_{C1} = 0.001$  V,  $a_{C2} = 0.0001$   $\Omega$ ,  $\theta_0 = 1 \cdot 10^{-5}$  s,  $\theta_1 = 2 \cdot 10^{-4}$  s,  $\alpha = 0.001$ ); (c) in the integral form with parameters ( $P_M = 500$  W,  $U_C = 80$  V,  $G_{1M} = 0.0001$  S,  $a_{M1} = 0.01$  V,  $a_{M2} = 0.01$   $\Omega$ ,  $a_{C2} = 0$   $\Omega$ ,  $\theta_0 = 1 \cdot 10^{-5}$  s,  $\theta_1 = 2 \cdot 10^{-4}$  s,  $\alpha = 0.001$ ); (d) in the integral form with parameters ( $P_M = 500$  W,  $U_C = 80$  V,  $G_{1M} = 0.0001$  S,  $a_{M1} = 0.01$  V,  $a_{M2} = 0.01$   $\Omega$ ,  $a_{C1} = 0$  V,  $\theta_0 = 1 \cdot 10^{-5}$  s,  $\theta_1 = 2 \cdot 10^{-4}$  s,  $\alpha = 0.001$ )

## 8. Conclusions

1. In the classic Mayr and Cassie mathematical models, rigorous simplifying assumptions are made that limit the applicability of these models for the approximation of the experimental characteristics of the electric arc.
2. The introduction of changes at the final stage of creating modified mathematical models of the electric arc causes violation of the basic input condition in the form of an energy balance.

3. When such changes are introduced at the initial stage of creating modified mathematical models of the electric arc, the basic input condition in the form of energy balance is not affected.
4. When modifications are introduced at the initial stage of creating the Mayr model using the residual conductance  $G_{M1}$  or the corresponding  $I_M$  current, it is possible to prescribe the ignition voltage.
5. When modifications are introduced at the initial stage of creating the Cassie model using the residual conductance  $G_{C1}$ , it is possible to reduce the arc ignition voltage to zero and at the same time to prescribe the angle of the tangent to the voltage-current characteristic at the beginning of the coordinate system.
6. Taking into account the phenomenon of increasing the power dissipated from an arc in the given ranges of plasma current variation will allow a better approximation of experimental data using modified mathematical models.
7. The hybrid model, combining modified Mayr and Cassie sub-models offers extended possibilities of the approximation of dynamic arc characteristics in a wide range of current variation.

## References

- [1] King-Jet Tseng, Yaoming Wang D., Mahinda Vilathgamuwa, *An experimentally verified hybrid Cassie-Mayr electric arc model for power electronics simulations*, IEEE Transactions on Power Electronics, vol. 12, no. 3, pp. 429–436 (1997), DOI: [10.1109/63.575670](https://doi.org/10.1109/63.575670).
- [2] Sawicki A., Haltof M., *Spectral and integral methods of determining parameters in selected electric arc models with a forced sinusoid current circuit*, Archives of Electrical Engineering, vol. 65, no. 1, pp. 87–103 (2016), DOI: [10.1515/ae-2016-0007](https://doi.org/10.1515/ae-2016-0007).
- [3] Pentegov I.V., Sidorec V.N., *Comparative analysis of models of dynamic welding arc*, The Paton Welding Journal, no. 12, pp. 45–48 (2015), DOI: [10.15407/tpwj2015.12.09](https://doi.org/10.15407/tpwj2015.12.09).
- [4] Kalasek V., *Measurements of time constants on cascade d.c. arc in nitrogen*, TH-Report 71-E18, Eindhoven, pp. 1–30 (1971).
- [5] Sawicki A., *The universal Mayr–Pentegov model of the electric arc*, Przegląd Elektrotechniczny (Electrical Review), vol. 94, no. 12, pp. 208–211 (2019), DOI: [10.15199/48.2019.12.47](https://doi.org/10.15199/48.2019.12.47).
- [6] Katsaounis A., *Heat flow and arc efficiency at high pressures in argon and helium tungsten arcs*, Welding Research Supplement I, September, pp. 447-s–454-s (1993).
- [7] Maximov S., Venegas V., Guardado J.L., Melgoza E., Torres D., *Asymptotic methods for calculating electric arc model parameters*, Electrical Engineering, vol. 94, no. 2, pp. 89–96 (2012), DOI: [10.1007/s00202-011-0214-6](https://doi.org/10.1007/s00202-011-0214-6).
- [8] Sawicki A., *Arc models for simulating processes in circuits with a SF<sub>6</sub> circuit breaker*, Archives of Electrical Engineering, vol. 68, no. 1, pp. 147–159 (2019), DOI: [10.24425/ae.2019.125986](https://doi.org/10.24425/ae.2019.125986).
- [9] Sawicki A., *Classical and Modified Mathematical Models of Electric Arc*, Institute of Welding Bulletin, no. 4, pp. 67–73 (2019), DOI: [10.17729/ebis.2019.4/7](https://doi.org/10.17729/ebis.2019.4/7).
- [10] Janowski T., Jaroszyński L., Stryczewska H.D., *Modification of the Mayr's electric arc model for gliding Arc Analysis*, XXVI International Conference on Phenomena in Ionized Gases, Nagoya, Japan 2001/7/17, pp. 341–342 (2001).
- [11] Ziani A., Moulai H., *Hybrid model of electric arcs in high voltage circuit breakers*, Electric Power Systems Research, vol. 92, pp. 37–42 (2012), DOI: [10.1016/j.epsr.2012.04.021](https://doi.org/10.1016/j.epsr.2012.04.021).